



Microwave photonic link to transmit four microwave vector signals on a single optical carrier based on coherent detection and digital signal processing

PENG LI,^{1,2} ZHENG DAI,¹  LIANSHAN YAN,²  AND JIANPING YAO^{1,*} 

¹Microwave Photonics Research Laboratory, School of Electrical Engineering and Computer Science, University of Ottawa, Ottawa, ON K1N 6N5, Canada

²Center for Information Photonics & Communications, School of Information Science & Technology, Southwest Jiaotong University, Chengdu, Sichuan 610031, China

*jpyao@uottawa.ca

Abstract: A microwave photonic link to transmit four independent microwave vector signals modulated on a single optical carrier based on coherent detection and digital signal processing (DSP) is proposed and experimentally demonstrated. At the transmitter, a continuous-wave (CW) light wave is modulated by four independent microwave vector signals with an identical center microwave frequency at a dual-polarization dual-drive Mach-Zehnder modulator (DP-DDMZM), to generate four intensity-modulated optical signals, with two signals sharing one of the two orthogonal polarization states. After transmission over a single-mode fiber (SMF), the optical signals are applied to a polarization- and phase- diversity coherent receiver to which a light wave from a second laser source as a local oscillator (LO) is also applied. To eliminate the joint phase noise and the unstable offset frequency from the transmitter and the LO laser sources and to perform polarization demultiplexing, a digital noise cancellation algorithm and a polarization demultiplexing algorithm are developed. The proposed approach is evaluated experimentally. For four independent 16 quadrature amplitude modulation (16-QAM) microwave vector signals at 4 GHz with a symbol rate of 0.5 GSymbol/s, error-free transmission over a 9-km SMF is achieved when the received optical power at the coherent receiver is higher than -21 dBm with forward error correction (FEC).

© 2022 Optica Publishing Group under the terms of the [Optica Open Access Publishing Agreement](#)

1. Introduction

Thanks to the low insertion loss, large bandwidth, and immunity to electromagnetic interference (EMI), radio over fiber (RoF), a technique to transmit microwave signals over an optical fiber link, has been considered one of the promising solutions for broadband wireless access networks [1–6]. To meet the requirement for higher data rate transmission, a RoF link with a high spectrum efficiency to maximize the use of the limited spectrum resources is expected. For example, in an intensity-modulation and direct-detection (IM-DD) RoF link, by imposing two independent data signals on the left sideband (LSB) and right sideband (RSB) of a double-sideband with carrier (DSB + C) optical signal, the data rate is doubled [7,8]. However, to enable correct detection with minimal cross-talks between the two data signals, two sharp cut-off optical bandpass filters (OBPFs) are used to separate the LSB and the RSB signals, making the system more complicated. In addition, the spectral efficiency is not doubled since the transmission of two sidebands required two times the bandwidth than the transmission of a single sideband. On the other hand, the spectral efficiency can be increased by using a coherent RoF link without using OBPFs [9,10]. In addition to a higher spectral efficiency, the receiver sensitivity of a coherent RoF link is also higher. The key challenge in implementing a coherent RoF link is the sensitivity of the receiver

to phase fluctuations including the joint phase noise and unstable offset frequency introduced by the transmitter and the local oscillator (LO) laser sources.

To solve the problem, digital signal processing (DSP) solutions should be employed. For example, we reported a coherent RoF link [11,12], in which the joint phase noise and unstable offset frequency were eliminated through DSP. After coherent detection, the joint phase noise was converted into an amplitude noise in two equal-amplitude quadrature signals. By summing the squared in-phase and quadrature components, the joint phase noise was fully eliminated [11,12]. The work in [11,12] was a demonstration to show the effectiveness of using DSP to eliminate the joint phase noise, but only a single microwave vector signal was transmitted. In fact, based on coherent detection, two or more microwave signals on a single optical carrier can be transmitted. In [13,14], a coherent RoF link to transmit two microwave signals with one being intensity modulated and the other phase modulated on a single optical carrier was reported. To ensure effective detection, one of the two orthogonal polarization states was used to transmit a pilot tone or a modulated optical signal. Since two orthogonal polarization states were employed, polarization multiplexing could not be implemented to further increase the spectral efficiency. In addition, at the receiver the two polarization-multiplexed optical signals were demultiplexed by manually adjusting a polarization controller (PC), which was not able to track the changes in the polarization, making the transmission performance decreased. To further improve the spectral efficiency, an approach to transmitting four microwave vector signals on a single optical carrier based on optical independent sideband modulation and optical orthogonal modulation was proposed [15]. Again, to ensure effective detection, two additional electrical pilot tones at different frequencies were employed, making the system have a reduced efficiency. Recently, we proposed an approach to transmitting two microwave vector signals on a single optical carrier with one polarization state based on coherent detection and digital phase noise cancellation [16]. A new DSP algorithm was developed, which was able to eliminate the joint phase noise and the unstable offset frequency. Two microwave vector signals were transmitted and recovered experimentally.

In this paper, to further increase the transmission capacity we propose an approach to transmitting four independent microwave vector signals on a single optical carrier with two orthogonal polarization states based on coherent detection and DSP. At the transmitter, a continuous-wave (CW) light wave generated by a transmitter laser is intensity-modulated by four independent microwave vector signals at a dual-polarization dual-drive Mach-Zehnder modulator (DP-DDMZM), to generate four intensity-modulated optical signals, with two signals sharing one of the two orthogonal polarization states. The polarization multiplexed optical signals are transmitted over a single-mode fiber (SMF) to a polarization- and phase- diversity coherent receiver to which the light wave from a second CW laser source as an LO is applied. A digital phase noise cancellation algorithm is developed and applied to eliminate the phase fluctuations including joint phase noise and unstable offset frequency introduced by the transmitter and the LO laser sources. To enable effective detection with full recovery of the four microwave vector signals, a constant module algorithm (CMA) is developed through which effective polarization demultiplexing is implemented. Since no manual control of the polarization states is needed, the system performance is improved. To verify the proposed scheme, an experiment is performed. Four independent 16 quadrature amplitude modulation (16-QAM) microwave vector signals at 4 GHz with a symbol rate of 0.5 GSymb/s are modulated on an optical carrier and transmitted over a 9-km SMF. After coherent detection and DSP, the four microwave vector signals are recovered. The transmission performance in terms of error vector magnitudes (EVMs) and bit error rates (BERs) is evaluated. The results show that when the received power is -21 dBm, the estimated BERs for the four recovered 16-QAM signals are 1.1×10^{-3} , 1.6×10^{-3} , 1.6×10^{-3} , and 1.9×10^{-3} , which enable error-free transmission with forward error correction (FEC).

2. Principle

Figure 1 shows the schematic diagram of the proposed RoF link for four microwave vector signal transmission based on coherent detection and DSP. At the transmitter, a laser diode (LD) is used as a transmitter laser source to generate a CW light wave which is sent to a DP-DDMZM via a PC (PC1). The DP-DDMZM is an integrated modulator consisting of a 3 dB optical coupler (OC), two sub-DDMZMs, a polarization rotator, and a polarization beam combiner (PBC). Both sub-DDMZMs are biased at the quadrature transmission point. Four independent microwave vector signals with an identical center frequency are applied to the DP-DDMZM via the four radio-frequency (RF) ports. At the output of the DP-DDMZM, four intensity-modulated optical signals, with two signals sharing one of the two orthogonal polarization states, are generated and transmitted over an SMF to a polarization- and phase-diversity coherent receiver. To perform coherent detection, the light wave from a second laser source serving as an LO is applied to the coherent receiver. At the output of the coherent receiver, four electrical signals are generated, which are sampled by an oscilloscope (OSC), and processed by a DSP unit.

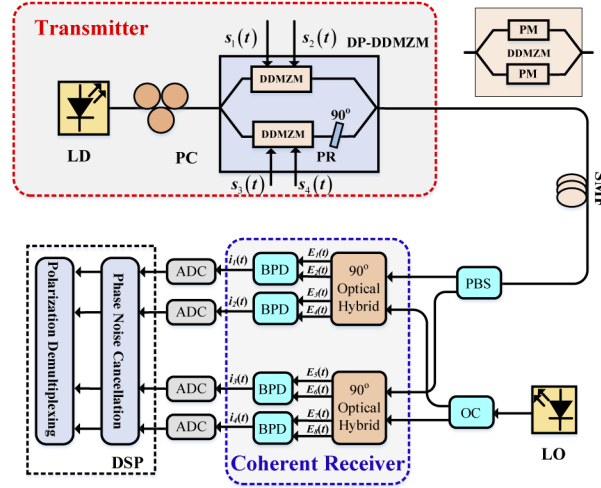


Fig. 1. Schematic diagram of the proposed RoF link for four independent vector signal transmission. LD: laser diode; PC: polarization controller; DDMZM: dual-drive Mach-Zehnder modulator; PR: polarization rotator; DP-DDMZM: dual-polarization dual-drive Mach-Zehnder modulator; SMF: single-mode fiber; LO: local oscillator; PBS: polarization beam splitter; OC: optical coupler; BPD: balanced photodetector; ADC: analog-to-digital converter; DSP: digital signal processing.

The four microwave vector signals with an identical center frequency are given by

$$s_i(t) = m_i(t) \cos(\omega_R t + \theta_i(t)) \quad (i = 1, 2, 3, 4) \quad (1)$$

where $m_i(t)$ and $\theta_i(t)$ are the amplitude and phase of the i -th microwave vector signal, and ω_R is the center angular frequency of the four microwave vector signals. In the system, both the sub-DDMZMs are biased at the quadrature transmission point. At the output of the DP-DDMZM, two orthogonally-polarized optical signals with each having two microwave vector signals are generated, which are given by [17]

$$\begin{aligned} E_x(t) &= \frac{\sqrt{P_s L}}{2} \exp j(\omega_c t + \varphi_c(t)) \times \left[\exp j \left(\frac{\pi}{V_\pi} s_1(t) \right) + \exp j \left(\frac{\pi}{V_\pi} s_2(t) + \frac{\pi}{2} \right) \right] \\ &\approx \frac{\sqrt{P_s L}}{2} \exp j(\omega_c t + \varphi_c(t)) \left(\frac{\pi}{V_\pi} (s_1(t) + j s_2(t)) + 1 + j \right) \end{aligned} \quad (2)$$

$$\begin{aligned}
 E_y(t) &= \frac{\sqrt{P_s L}}{2} \exp j(\omega_c t + \varphi_c(t)) \times \left[\exp j \left(\frac{\pi}{V_\pi} s_3(t) \right) + \exp j \left(\frac{\pi}{V_\pi} s_4(t) + \frac{\pi}{2} \right) \right] \\
 &\approx \frac{\sqrt{P_s L}}{2} \exp j(\omega_c t + \varphi_c(t)) \left(\frac{\pi}{V_\pi} (s_3(t) + j s_4(t)) + 1 + j \right)
 \end{aligned} \quad (3)$$

where P_s is the optical power of the light wave at the output of the transmitter laser source, L is the link loss between the transmitter laser and the DP-DDMZM, ω_c is the angular frequency of the light wave, $\varphi_c(t)$ is the phase noise term of the light wave from the transmitter laser source, and V_π is the half-wave voltage of the DP-DDMZM. As can be seen from Eqs. (2) and (3), microwave vector signals $s_1(t)$ and $s_2(t)$ are linearly mapped to the optical domain with a phase shift of 90° with the X-polarization state; while $s_3(t)$ and $s_4(t)$ are mapped to the optical domain with a phase shift 90° with the Y-polarization state. The orthogonally-polarized optical signals are transmitted over the SMF to a polarization- and phase- diversity coherent receiver which consists of a polarization beam splitters (PBS), a 3-dB OC, two 90° optical hybrids, and four balanced photodetectors (BPDs). To perform coherent detection, a free-running CW light wave generated by a second LD serving as the LO laser source is applied to the coherent receiver. The optical field at the output of the LO laser source is given by

$$E_{LO}(t) = \sqrt{P_{LO}} \exp j(\omega_{LO} t + \varphi_{LO}(t)) \quad (4)$$

where P_{LO} is the optical power of the light wave at the output of the LO laser source, ω_{LO} is the angular frequency of the light wave, and $\varphi_{LO}(t)$ is the phase noise term of the light wave from the LO laser source. After passing the two 90° optical hybrids, eight optical signals are obtained, which are given by

$$E_1(t) = E_x(t) \cos \alpha + E_y(t) \sin \alpha + \frac{\sqrt{2}}{2} E_{LO}(t) \quad (5)$$

$$E_2(t) = E_x(t) \cos \alpha + E_y(t) \sin \alpha - \frac{\sqrt{2}}{2} E_{LO}(t) \quad (6)$$

$$E_3(t) = E_x(t) \cos \alpha + E_y(t) \sin \alpha + j \frac{\sqrt{2}}{2} E_{LO}(t) \quad (7)$$

$$E_4(t) = E_x(t) \cos \alpha + E_y(t) \sin \alpha - j \frac{\sqrt{2}}{2} E_{LO}(t) \quad (8)$$

$$E_5(t) = E_x(t) \sin \alpha - E_y(t) \cos \alpha + \frac{\sqrt{2}}{2} E_{LO}(t) \quad (9)$$

$$E_6(t) = E_x(t) \sin \alpha - E_y(t) \cos \alpha - \frac{\sqrt{2}}{2} E_{LO}(t) \quad (10)$$

$$E_7(t) = E_x(t) \sin \alpha - E_y(t) \cos \alpha + j \frac{\sqrt{2}}{2} E_{LO}(t) \quad (11)$$

$$E_8(t) = E_x(t) \sin \alpha - E_y(t) \cos \alpha - j \frac{\sqrt{2}}{2} E_{LO}(t) \quad (12)$$

where α is the polarization angle between the X-polarization state and one principle axis of the PBS. Then, the optical signals are detected at the BPDs and the photocurrents are given by

$$\begin{aligned}
 i_1(t) &= \frac{1}{2}R(E_1(t)E_1^*(t) - E_2(t)E_2^*(t)) \\
 &= \frac{R\sqrt{2P_sLP_{LO}}(\cos\alpha + \sin\alpha)}{4}(\cos[\Delta\omega t + \varphi(t)] - \sin[\Delta\omega t + \varphi(t)]) + \\
 &\quad \frac{\pi R\sqrt{2P_sLP_{LO}}}{4V\pi} \times \left(\cos\alpha \begin{pmatrix} s_1(t)\cos[\Delta\omega t + \varphi(t)] \\ -s_2(t)\sin[\Delta\omega t + \varphi(t)] \end{pmatrix} + \sin\alpha \begin{pmatrix} s_3(t)\cos[\Delta\omega t + \varphi(t)] \\ -s_4(t)\sin[\Delta\omega t + \varphi(t)] \end{pmatrix} \right) \quad (13)
 \end{aligned}$$

$$\begin{aligned}
 i_2(t) &= \frac{1}{2}R(E_3(t)E_3^*(t) - E_4(t)E_4^*(t)) \\
 &= \frac{R\sqrt{2P_sLP_{LO}}(\cos\alpha + \sin\alpha)}{4}(\sin[\Delta\omega t + \varphi(t)] + \cos[\Delta\omega t + \varphi(t)]) + \\
 &\quad \frac{\pi R\sqrt{2P_sLP_{LO}}}{4V\pi} \left(\cos\alpha \begin{pmatrix} s_1(t)\sin[\Delta\omega t + \varphi(t)] \\ +s_2(t)\cos[\Delta\omega t + \varphi(t)] \end{pmatrix} + \sin\alpha \begin{pmatrix} s_3(t)\sin[\Delta\omega t + \varphi(t)] \\ +s_4(t)\cos[\Delta\omega t + \varphi(t)] \end{pmatrix} \right) \quad (14)
 \end{aligned}$$

$$\begin{aligned}
 i_3(t) &= \frac{1}{2}R(E_5(t)E_5^*(t) - E_6(t)E_6^*(t)) \\
 &= \frac{R\sqrt{2P_sLP_{LO}}(\sin\alpha - \cos\alpha)}{4}(\cos[\Delta\omega t + \varphi(t)] - \sin[\Delta\omega t + \varphi(t)]) + \\
 &\quad \frac{\pi R\sqrt{2P_sLP_{LO}}}{4V\pi} \left(\sin\alpha \begin{pmatrix} s_1(t)\cos[\Delta\omega t + \varphi(t)] \\ -s_2(t)\sin[\Delta\omega t + \varphi(t)] \end{pmatrix} - \cos\alpha \begin{pmatrix} s_3(t)\cos[\Delta\omega t + \varphi(t)] \\ -s_4(t)\sin[\Delta\omega t + \varphi(t)] \end{pmatrix} \right) \quad (15)
 \end{aligned}$$

$$\begin{aligned}
 i_4(t) &= \frac{1}{2}R(E_7(t)E_7^*(t) - E_8(t)E_8^*(t)) \\
 &= \frac{R\sqrt{2P_sLP_{LO}}(\sin\alpha - \cos\alpha)}{4}(\sin[\Delta\omega t + \varphi(t)] + \cos[\Delta\omega t + \varphi(t)]) + \\
 &\quad \frac{\pi R\sqrt{2P_sLP_{LO}}}{4V\pi} \left(\sin\alpha \begin{pmatrix} s_1(t)\sin[\Delta\omega t + \varphi(t)] \\ +s_2(t)\cos[\Delta\omega t + \varphi(t)] \end{pmatrix} - \cos\alpha \begin{pmatrix} s_3(t)\sin[\Delta\omega t + \varphi(t)] \\ +s_4(t)\cos[\Delta\omega t + \varphi(t)] \end{pmatrix} \right) \quad (16)
 \end{aligned}$$

where R is the responsivity of the BPDs, $\Delta\omega = \omega_c - \omega_{LO}$ is the offset frequency between the light waves from the transmitter and the LO laser sources, and $\varphi(t)$ is the joint phase noise of the two laser sources. It can be seen from Eqs. (13) to (16), the four currents contain two terms. The first term is the phase fluctuations, including the joint phase noise and the unstable offset frequency between the transmitter laser source and LO laser source, while the second term contains the four microwave vector signals, which are affected by the phase fluctuations. If the frequency difference between the two laser sources is lower than the center frequency of the microwave vector signal, which is true considering the microwave carrier frequency is much higher than the offset frequency, the two terms can be easily separated by a digital filter.

To eliminate the joint phase noise and unstable offset frequency introduced by the two laser sources, a novel digital phase noise cancellation algorithm is developed. The flow charts to show the algorithm are given in Figs. 2(a)-(d). The first terms ($i_{12}(t)$, $i_{22}(t)$, $i_{32}(t)$, and $i_{42}(t)$) in each of the currents ($i_1(t)$, $i_2(t)$, $i_3(t)$, and $i_4(t)$) are obtained via a digital low-pass filter (LPF), while the second terms ($i_{11}(t)$, $i_{21}(t)$, $i_{31}(t)$, and $i_{41}(t)$) are obtained by using a digital bandpass filter

(BPF). The detailed signal processing algorithm can be expressed by the following expressions

$$i_5(t) = (i_{12}(t) + i_{22}(t))*i_{11}(t) + (i_{22}(t) - i_{12}(t))*i_{21}(t) \tag{17}$$

$$= \frac{\pi P_s LP_{LO} R^2}{4V_\pi} (\cos \alpha + \sin \alpha) \times (\cos \alpha s_1(t) + \sin \alpha s_3(t))$$

$$i_6(t) = (i_{12}(t) + i_{22}(t))*i_{21}(t) - (i_{22}(t) - i_{12}(t))*i_{11}(t) \tag{18}$$

$$= \frac{\pi P_s LP_{LO} R^2}{4V_\pi} (\cos \alpha + \sin \alpha) \times (\cos \alpha s_2(t) + \sin \alpha s_4(t))$$

$$i_7(t) = (i_{32}(t) + i_{42}(t))*i_{31}(t) + (i_{42}(t) - i_{32}(t))*i_{41}(t) \tag{19}$$

$$= \frac{\pi P_s LP_{LO} R^2}{4V_\pi} (\sin \alpha - \cos \alpha) \times (\sin \alpha s_1(t) - \cos \alpha s_3(t))$$

$$i_8(t) = (i_{32}(t) + i_{42}(t))*i_{41}(t) - (i_{42}(t) - i_{32}(t))*i_{31}(t) \tag{20}$$

$$= \frac{\pi P_s LP_{LO} R^2}{4V_\pi} (\sin \alpha - \cos \alpha) \times (\sin \alpha s_2(t) - \cos \alpha s_4(t))$$

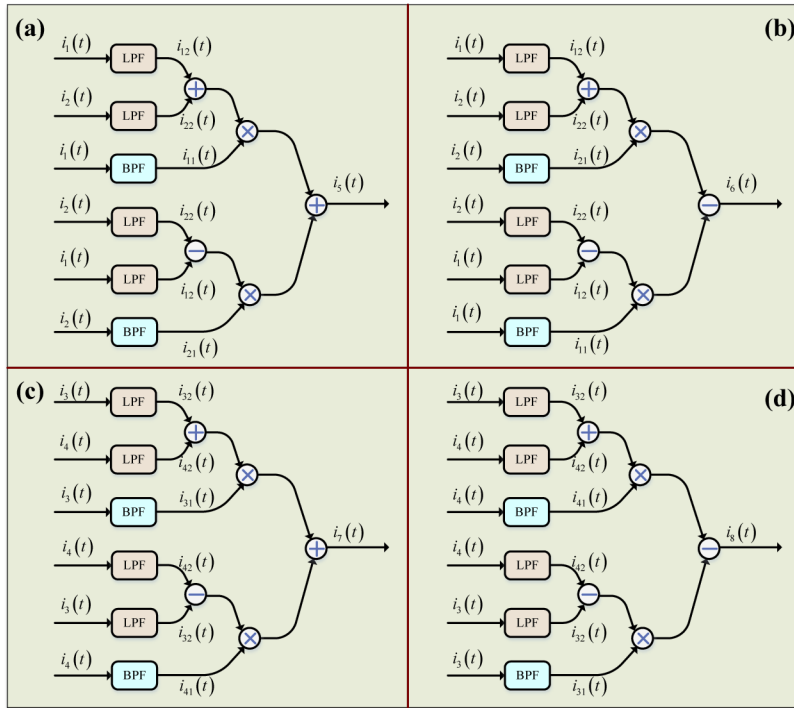


Fig. 2. Flow charts to show the algorithm to eliminate the joint phase noise and unstable offset frequency (a) $i_5(t)$, (b) $i_6(t)$, (c) $i_7(t)$, and (d) $i_8(t)$. LPF: low-pass filter; BPF: bandpass filter.

It can be seen the obtained two signals, $i_5(t)$ and $i_7(t)$ in Eqs. (17) and (19), are functions of $s_1(t)$, $s_3(t)$ and the polarization angle α , but are free from the joint phase noise and unstable offset frequency. By employing a CMA for polarization demultiplexing [18,19], the two microwave vector signals, $s_1(t)$ and $s_3(t)$, can be recovered. Similarly, $i_6(t)$ and $i_8(t)$ in Eqs. (18) and (20), are functions of $s_2(t)$ and $s_4(t)$, and the polarization angle α . Again, by employing a CMA for polarization demultiplexing, $s_2(t)$ and $s_4(t)$, can also be recovered.

3. Experimental setup and results

To validate the operation of the proposed RoF link, a proof-of-concept experiment based on the setup as shown in Fig. 1 is conducted. At the transmitter, a laser source (Yokogawa, AQ2201) is used as the transmitter laser source. A CW light wave at 1550 nm generated by the laser source with a power of 8 dBm and a linewidth of 100 kHz is sent to a DP-DDMZ (Fujitsu, FTM7980EDA) via PC1. Note that PC1 is used to minimize the polarization-dependent loss (PDL). The DP-DDMZ has a bandwidth of 21.5 GHz and a half-wave voltage of 3.5 V (the half-wave voltage of the two sub-DDMZs is also 3.5 V). Four independent 16-QAM microwave vector signals with a center frequency of 4 GHz and a baud rate of 0.5 GSym/s are generated by an arbitrary waveform generator (AWG, Keysight M8195A) with a sampling rate of 65 GSa/s and a bandwidth of 25 GHz and are applied to the DP-DDMZ via the four RF ports. Both sub-DDMZs are biased at the quadrature transmission point. At the output of the DP-DDMZ, two orthogonally-polarized optical signals with one having two microwave vector signals are generated and transmitted over a 9-km SMF to a polarization- and phase- diversity coherent receiver (Keysight N4391A) with a bandwidth of 40 GHz via the optical signal input port. At the receiver, a second laser source (Agilent N7714A) is used as the LO laser source to generate a second CW light wave at 1550.005 nm with a power of 12 dBm and a linewidth of 100 kHz, which is also applied to the coherent receiver via the LO optical port. Note that the polarization states of the modulated optical signal and LO optical signal at the input of the coherent receiver are arbitrary. Four electrical signals at the output of the coherent receiver are generated, which are sampled by a digital storage oscilloscope (Agilent DSO-Z 504A) with a bandwidth of 50 GHz and a sampling rate of 160 GSa/s, and then processed by a DSP unit.

Figure 3(a) shows the measured spectrum of the electrical signal at one of the four outputs of the coherent receiver ($i_1(t)$). It can be seen a low-frequency microwave signal around 0.6 GHz is generated due to the frequency difference between the transmitter laser source and the LO laser source. In addition, two microwave signals at 3.4 GHz and 4.6 GHz with a bandwidth of 0.5 GHz are observed due to the mixing between the 0.6 GHz microwave signal and the 4 GHz microwave vector signals. The 0.6 GHz microwave signal can be obtained from $i_1(t)$ by using an LPF, as

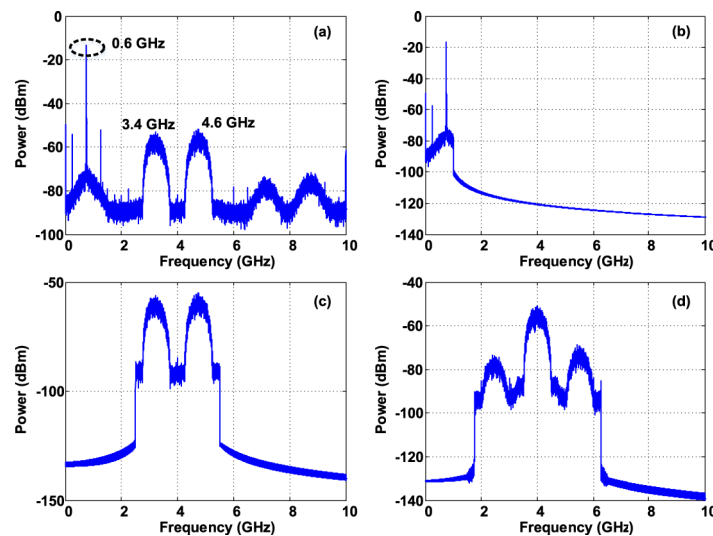


Fig. 3. The measured spectral of the electrical signals (a) at the first output port of the coherent receiver ($i_1(t)$), (b) at the output of an LPF ($i_{12}(t)$), (c) at the output of a BPF ($i_{11}(t)$) and (d) at the output of the DSP unit after digital phase noise cancellation ($i_5(t)$).

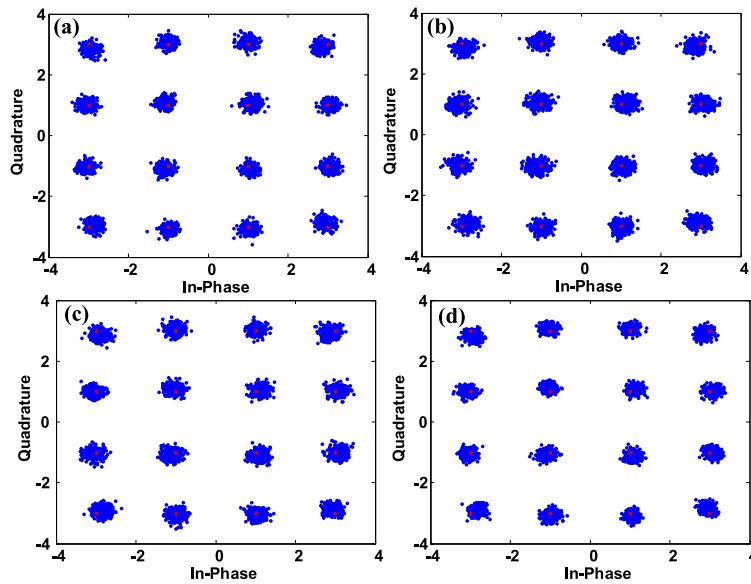


Fig. 4. Measured constellations of the four recovered 16-QAM microwave vector signals at the output of the DSP unit (fiber length: 9 km, the received optical power: -13 dBm). (a) $s_1(t)$, (b) $s_2(t)$, (c) $s_3(t)$, and (d) $s_4(t)$.

shown in Fig. 3(b). The two microwave signals at 3.4 GHz and 4.6 GHz can be separated from $i_1(t)$ by using a BPF, as shown in Fig. 3(c). Through digital phase noise cancellation, two mixed microwave vector signals $s_1(t)$ and $s_3(t)$ free from the joint phase noise and the unstable offset frequency are achieved, as shown in Fig. 3(d). To fully recover the microwave vector signals, a CMA is used for polarization demultiplexing. Figure 4 shows the measured constellations of the four fully recovered microwave vector signals at the output of the DSP unit, where the optical power at the input of the coherent receiver is -13 dBm. It can be seen that the four microwave vector signals are completely recovered.

To further evaluate the performance of the system, the EVMs for the four recovered microwave vector signals at different received optical power levels are also measured, as shown in Figs. 5(a). Based on the EVMs, the BERs are estimated, as shown in Fig. 5(b). When calculating the BERs,

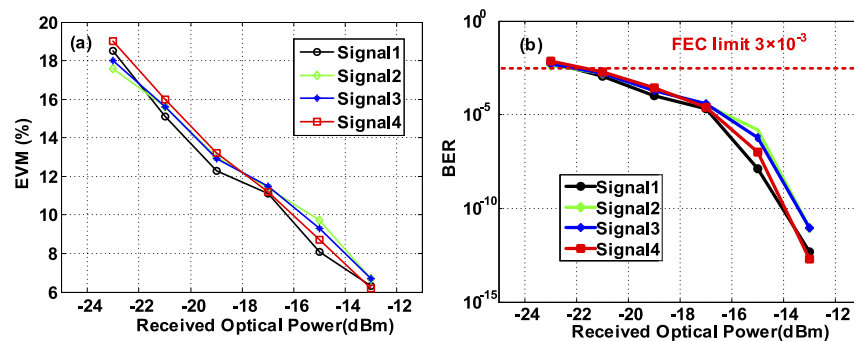


Fig. 5. (a) Measured EVMs and (b) estimated BERs at different received optical power levels for the four recovered 16-QAM microwave vector signals transmitted over a 9-km SMF.

we assume that the noise after the DSP unit is a stationary random process with Gaussian statistics [20–22]. It can be seen when the received optical power is -13 dBm, the EVMs for the four recovered 16-QAM microwave vector signals are 6.3%, 6.7%, 6.7%, and 6.2% and the estimated BERs are 4.7×10^{-13} , 9.3×10^{-13} , 9.3×10^{-13} , and 2.1×10^{-13} , which are far below the FEC limit. When the optical power is decreased to -21 dBm, the estimated BERs are 1.1×10^{-3} , 1.6×10^{-3} , 1.6×10^{-3} , and 1.9×10^{-3} , which are well within the FEC limit. When the optical power is further decreased to -23 dBm, the estimated BERs are 5.9×10^{-3} , 4.1×10^{-3} , 4.9×10^{-3} , and 7.0×10^{-3} , which are beyond the FEC limit. By employing a state-of-the-art FEC technique, a raw BER of up to 3×10^{-3} can be improved to an effective BER of 1×10^{-15} at the expense of a 6.7% overhead [23]. Therefore, when the optical power is higher than -21 dBm, error-free transmission can be achieved.

4. Conclusion

We have proposed and experimentally demonstrated a coherent RoF link to transmit four independent microwave vector signals modulated on one single optical carrier based on coherent detection and DSP. At the transmitter, four independent microwave vector signals were modulated on one single optical carrier via a DP-DDMZM with two microwave vector signals sharing one of the two orthogonal polarization states. At the output of the DP-DDMZM, two polarization multiplexed optical signals with one having two microwave vector signals were generated, which were transmitted over an SMF, and detected at a polarization- and phase- diversity coherent receiver, to which a free-running CW light wave from an LO laser source was applied. By using the digital phase noise cancellation algorithm and polarization demultiplexing algorithm, the four microwave vector signals free from the joint phase noise and unstable offset frequency were recovered. An experiment was conducted. The transmission of four independent microwave vector signals at 4 GHz with a symbol rate of 0.5 GSymb/s over a 9-km SMF link was demonstrated. The transmission performance of the RoF link in terms of EVMs and BERs was also evaluated. When the received power was -21 dBm, the estimated BERs for the four recovered 16-QAM signals were 1.1×10^{-3} , 1.6×10^{-3} , 1.6×10^{-3} , and 1.9×10^{-3} . With FEC, error-free transmission is still enabled.

Funding. Natural Sciences and Engineering Research Council of Canada; National Research Council Canada.

Disclosures. The authors declare no conflicts of interest.

Data availability. Data underlying the results presented in this paper are not publicly available at this time but may be obtained from the authors upon reasonable request.

References

1. A. Seeds and K. Williams, "Microwave photonics," *J. Lightwave Technol.* **24**(12), 4628–4641 (2006).
2. C. Cox, E. Ackerman, G. Betts, and J. Prince, "Limits on the performance of RF-over-fiber links and their impact on device design," *IEEE Trans. Microwave Theory Tech.* **54**(2), 906–920 (2006).
3. J. Capmany and D. Novak, "Microwave photonics combines two worlds," *Nature Photon.* **1**(6), 319–330 (2007).
4. J. Yao, "Microwave photonics," *J. Lightwave Technol.* **27**(3), 314–335 (2009).
5. J. Beas, G. Castanon, I. Aldaya, A. Zavala, and G. Campuzano, "Millimeter-wave frequency radio over fiber systems: A survey," *IEEE Commun. Surv. Tuts.* **15**(4), 1593–1619 (2013).
6. X. Li, Z. Dong, J. Yu, N. Chi, Y. Shao, and G. Chang, "Fiber-wireless transmission system of 108 Gb/s data over 80 km fiber and 2x2 multiple-input multiple-output wireless links at 100 GHz W-band frequency," *Opt. Lett.* **37**(24), 5106–5108 (2012).
7. X. Pan, X. Liu, H. Zhang, K. Wang, Y. Zhang, D. Ran, X. Wang, and C. Wang, "Independent dual single-sideband vector millimeter-wave signal generation by one single I/Q modulator," *Opt. Express* **27**(14), 19906–19914 (2019).
8. R. Deng, J. Yu, J. He, M. Chen, Y. Wei, L. Zhao, Q. Zhang, and X. Xin, "Twin-SSB-OFDM transmission over heterodyne W-band fiber-wireless system with real-time implementable blind carrier recovery," *J. Lightwave Technol.* **36**(23), 5562–5572 (2018).
9. K. Kitayama, A. Maruta, and Y. Yoshida, "Digital coherent technology for optical fiber and radio-over-fiber transmission systems," *J. Lightwave Technol.* **32**(20), 3411–3420 (2014).
10. G. Agrawal, *Fiber-Optic Communication Systems*, 3rd ed. Wiley, Hoboken, NJ, USA, 478–517 (2002).

11. X. Chen and J. Yao, "A coherent microwave photonic link with digital phase noise cancellation," in *Proc. Int. Topical Meeting Microw. Photon.* 438–441 (2014).
12. X. Chen, T. Shao, and J. Yao, "Digital phase noise cancellation for a coherent-detection microwave photonic link," *IEEE Photonics Technol. Lett.* **26**(8), 805–808 (2014).
13. X. Chen and J. Yao, "A high spectral efficiency coherent microwave photonic link employing both amplitude and phase modulation with digital phase noise cancellation," *J. Lightwave Technol.* **33**(14), 1 (2015).
14. H. Zhang, A. Wen, W. Zhang, W. Zhang, W. Zhai, and Z. Tu, "A novel spectral-efficient coherent radio-over-fiber link with linear digital-phase demodulation," *IEEE Photonics J.* **12**(1), 1–8 (2020).
15. X. Chen and J. Yao, "4×4 multiple-input multiple-output coherent microwave photonic link with optical independent sideband and optical orthogonal modulation (invited paper)," *Chin. Opt. Lett.* **15**(1), 1–7 (2017).
16. P. Li, R. Xu, Z. Dai, Z. Lu, L. Yan, and J. P. Yao, "A high spectral efficiency radio over fiber link based on coherent detection and digital phase noise cancellation," *J. Lightwave Technol.* **39**(20), 6443–6449 (2021).
17. L. Zhang, Q. Zhang, T. Zuo, E. Zhou, G. Liu, and X. Xu, "C-band single wavelength 100-Gb/s IM-DD transmission over 80-km SMF without CD compensation using SSB-DMT," In *Proc. Opt. Fiber Commun.* Los Angeles, CA, USA, 2015, Paper Th4A.2.
18. A. Leven, N. Kaneda, and Y. Chen, "Real-time CMA-based 10 Gb/s polarization demultiplexing coherent receiver implemented in an FPGA," in *Proc. OFC/NFOEC'08*, San Diego, CA, USA, 24–28 (2008).
19. I. Roudas, A. Vgenis, C. Petrou, D. Toumpakaris, J. Hurley, M. Sauer, J. Downie, Y. Mauro, and S. Raghavan, "Optimal polarization demultiplexing for coherent optical communications systems," *J. Lightwave Technol.* **28**(7), 1121–1134 (2010).
20. D. H. Wolaver, "Measure error rates quickly and accurately," *Electron. Des.* **43**(11), 89–98 (1995).
21. A. Brillant, *Digital and Analog Fiber Optic Communication for CATV and FTTx Applications*. SPIE: Bellingham, WA, USA, 653–660 (2008).
22. V. J. Urick, J. X. Qiu, and F. Bucholtz, "Wide-band QAM-over-fiber using phase modulation and interferometric demodulation," *IEEE Photonics Technol. Lett.* **16**(10), 2374–2376 (2004).
23. R. Schmogrow, D. Hillerkuss, S. Wolf, B. Bauerle, M. Winter, P. Kleinow, B. Nebendahl, T. Dippon, P. C. Schindler, C. Koos, W. Freude, and J. Leuthold, "512QAM Nyquist Sinc-pulse transmission at 54 Gbit/s in an optical bandwidth of 3 GHz," *Opt. Express* **20**(6), 6439–6447 (2012).